Accumulation of circulating CCR7^{+} natural killer cells marks melanoma evolution and reveals a CCL19-dependent metastatic pathway.

Costanza Maria Cristiani[1δ], Alice Turdo[2δ], Valeria Ventura[1,7], Tiziana Apuzzo[2], Mariaelena Capone[3], Gabriele Madonna[3], Domenico Mallardo[3], Cinzia Garofalo[1], Emilia Dora Giovannone[4], Antonio M. Grimaldi[3], Rossana Tallerico[1], Emanuela Marcenaro[5], Silvia Pesce[5], Genny Del Zotto[6], Valter Agosti[1,4], Francesco Saverio Costanzo[1,4], Elio Gulletta[7], Aroldo Rizzo[8], Alessandro Moretta[5], Klas Karre[9], Paolo A. Ascierto[3], Matilde Todaro[10*], and Ennio Carbone[1,9*]

[1]*Department of Experimental and Clinical Medicine, University "Magna Graecia" of Catanzaro, 88100 Catanzaro, Italy*
[2]*Department of Surgical, Oncological and Stomatological Sciences (Di.Chir.On.S), University of Palermo, 90127 Palermo, Italy*
[3]*Istituto Nazionale Tumori – IRCCS – Fondazione "G. Pascale",Dipartimento di Melanoma, Immunoterapia Oncologica e Terapie Innovative, 80131 Naples, Italy*
[4]*Services and Research Interdepartmental Center, University "Magna Graecia" of Catanzaro, 88100 Catanzaro, Italy*
[5]*Department of Experimental Medicine and Centre of Excellence for Biomedical Research, University of Genoa, 16132 Genoa, Italy*
[6]*Core Facilities Laboratory, Department of Translational Research, Laboratory Medicine, Diagnosis and Services, Istituto Giannina Gaslini, 16147 Genoa, Italy*
[7]*Department of Health Sciences, University "Magna Graecia" of Catanzaro, 88100 Catanzaro, Italy*
[8] *Unit of Pathology, Ospedali Riuniti Villa Sofia-Cervello, 90127 Palermo, Italy*
[9] *Department of Microbiology, Cell and Tumor biology, Karolinska Intitutet, SE-17176 Stockholm, Sweden*
[10]*Department of PROMISE, University of Palermo, 90127 Palermo, Italy*
[δ] *These authors contributed equally*

Running title
NK and CSC in melanoma metastasis: the CCR7-CCL19 axis role.

Keywords
Melanoma; immune surveillance; NK cells; cancer stem cells; metastasis;

Financial support
This work was supported by grants to E. Carbone from the Italian Association for Cancer Research (IG15521); Wenner-Gren Stiftelserna, Sweden; Italian Ministry of Health grant "Progetto Ricerca Finalizzata 2011–2012"; grant CO-2011–02348049 co-funded by Bristol Myers Squibb, Fondazione Melanoma Onlus, Naples; E. Marcenaro from AIRC-Special Program Metastatic disease: the key unmet need in oncology 5 per mille 2018 (21147) and Progetto Roche Ricerca 2017. M. Todaro received funding from the Italian Association for Cancer Research (IG14415) and (PSN) 2015- Linea Progettuale 6, Azione 6.2,CUP I76J17000470001. P. A. Ascierto was supported by Italian Ministry of Health "Ricerca Corrente". G. Madonna was supported by Institutional Project "Ricerca Corrente" Fondazione "G. Pascale"

***Corresponding authors**
Ennio Carbone (email: ennio.carbone@ki.se) and Matilde Todaro (email: matilde.todaro@gmail.com)

Conflict of interest disclosure statement
The authors have declared that no conflict of interest exists.

Abstract

Immune checkpoint blockade therapy has changed prognoses for many melanoma patients. However, immune responses that correlate with clinical progression of the disease are still poorly understood. To identify immune responses correlating with melanoma clinical evolution, we analyzed serum cytokines as well as circulating NK and T cell subpopulations from melanoma patients. The patients' immune profiles suggested that melanoma progression leads to changes in peripheral blood NK and T cell subsets. Stage IV melanoma was characterized by an increased frequency of $CCR7^{+}CD56^{bright}$ NK cells as well as high serum concentrations of the CCR7-ligand CCL19. CCR7 expression and CCL19 secretion were also observed in melanoma cell lines. The $CCR7^{+}$ melanoma cell subpopulation co-expressed PD-L1 and Galectin-9 and had stemness properties. Analysis of melanoma-derived cancer stem cells (CSCs) showed high CCR7 expression; these CSCs were efficiently recognized and killed by NK cells. An accumulation of $CCR7^{+}$, $PD\text{-}L1^{+}$ and $Galectin\text{-}9^{+}$ melanoma cells in melanoma metastases was demonstrated *ex vivo*. Altogether, our data identify biomarkers that may mark a CCR7-driven metastatic melanoma pathway.

Introduction

Immune checkpoint therapy has changed prognoses for many melanoma patients, increasing their overall survival (1,2). These successes in melanoma therapy have emphasized the role of the immune response in controlling tumor burden. Temporal cascades of gene mutations characterize the natural history of melanoma from the appearance of the early malignant nevus to its metastatic systemic spread (3). However, less is known regarding changes in the immune response as the disease progresses. Analysis of circulating T and NK cells during melanoma progression may identify prognostic biomarkers that could be assayed through patient liquid biopsies and mark disease progression.

Most melanoma patients at diagnosis have already developed local or disseminated lymph node (LN) metastases, but do not have visceral metastases. Prognoses for melanoma patients with early stage disease (II, III) are more favorable than prognoses for patients with stage IV disease. Self-renewing cancer stem cells (CSCs) are thought to be responsible for metastatic spread (4-6). CSCs express chemokine receptors that are involved in CSC phenotype promotion and/or maintenance (7).

NK cells, members of the Innate Lymphoid Cell group 1 (ILC1) family (8), are the most abundant ILC population found in circulating blood. NK cells are cytotoxic lymphocytes that have little effect on primary tumor lesions (9-11) but can control solid tumor metastatic spread (12). NK cell recognition of melanoma cells has been reported both *in vitro* and *in vivo* (13-15). Human NK cells are regulated by activating and inhibitory receptors. Activating receptors include NCRs (NKp30, NKp44 and NKp46), NKG2D and DNAM-1 that recognize stress inducible molecules expressed on the tumor cell surface. Inhibitory receptors are mainly HLA-class I recognizing KIRs that induce NK cell tolerance (16). In humans, circulating NK cells fall into two subsets, $CD56^{bright}$ and $CD56^{dim}$ NK cells (17). The proportions of the two subsets varies with anatomical localization (16). $CD56^{bright}$ NK cells prevail in secondary lymphoid organs and uterus, produce cytokines and have low cytotoxic potential. $CD56^{dim}$ NK cells are effector cells that lyse cancer and virus-infected cells. Moreover, $CD56^{dim}$ NK cells derived from individuals previously exposed to pathogens, such as human cytomegalovirus (HCMV), may include “memory-like” NK cells (18). Unknown cofactors associated with HCMV infection may induce the onset of a fully mature NK cell subset that is characterized by expression of the inhibitory checkpoint protein PD-1 (19).

Much is known about the regulation of NK cell-mediated cytotoxicity (20). NK cells selectively recognize melanoma metastatic cell lines (14) derived from tumor infiltrated lymph nodes. We showed that the presence of $CD57^{+}KIR^{+}CCR7^{+}CD3^{-}$ NK cells in melanoma-infiltrated lymph

nodes exerts an autologous anti-melanoma cytotoxicity the frequency of such cells may predict patient survival (21). The NK cell subset repertoire provides a number of variables that are associated with melanoma patients' response to anti immune checkpoint treatment with ipilimumab (22). We and others demonstrated that NK cells are able to control CSC mediated lung metastasis (23-25). To better elucidate the immune pathogenesis of melanoma, we here analyze circulating NK and T cells subpopulations, as defined by receptor expression, in the context of melanoma. We focused particularly on cell subsets expressing chemokine receptors that control cell migration and the cyto-chemokine serum environment. Our objective was to understand changes in the immune response associated with melanoma clinical evolution. Our investigations led to insights concerning the chemokine biology of melanoma cells, particularly a subpopulation of melanoma cells that are cancer stem cells. Altogether, our results suggest a role for the CCR7-CCL19 pathway during melanoma progression, in that a subpopulation of tumor cells may exploit the immune system through chemokine signaling.

Materials and Methods

Melanoma patients

For the characterization of changes happening in T and NK cell compartments in melanoma patients during disease progression, 166 melanoma patients (42 stage III and 124 stage IV melanoma patients) were enrolled in Italy at the NCI Fondazione "G. Pascale" of Naples and 24 stage IV melanoma patients were recruited at the Oncology clinic Karolinska University Hospital, Stockholm, Sweden. For each patient cohort, Ethical Committees associated with NCI of Naples, and Karolinska University Hospital, Stockholm granted ethical permission. Written informed consent was obtained from all patients in accordance with the Declaration of Helsinki for the use of human biological samples for research purposes. Stage III melanoma patients did not receive any treatment at the time of the enrollment, whereas stage IV were naïve or had been subjected to different types of chemotherapy. For lymphocyte compartment analysis and functional assays, peripheral blood mononuclear cells (PBMCs) were isolated from 80 and 29 patients, respectively. Cytokine quantification was performed on 88 patients.

PMBCs from 42 persons and sera from 9 persons, all sex- and age-matched healthy donors, were also isolated as controls at the Pugliese-Ciaccio Hospital and University Magna Graecia of Catanzaro, Catanzaro, Italy. The experiments were performed once per patient.

Isolation of peripheral blood lymphocytes and NK cell tumor cell lines

PBMCs from 80 melanoma patients and 42 healthy donors were isolated by Biocoll separating solution (Biochrom AG, Berlin, Germany) density gradient centrifugation. For functional experiments requiring NK cells, these cells were isolated from healthy donor PBMCs using human NK Cell Isolation Kit (Miltenyi Biotech, San Diego, CA, USA) according to manufacturer's instructions. The purity of isolated NK cells was > 95%, as assayed by flow cytometry.

Cell lines

K562, Huh7, a2780, RKO and HDFa cell lines were obtained from ATCC in 2013 (RKO and K562), 2014 (Huh7), 2015 (HDFa) and 2016 (a2780). Melanoma cell lines were obtained, based on informed consent, from surgical melanoma specimens of patients admitted at the Fondazione IRCCS Istituto Nazionale dei Tumori, Milan (2009), Istituto Nazionale Tumori - IRCCS "Fondazione G. Pascale", Naples (2018), and San Raffaele University Hospital, Milan (2013) (Supplementary Table S1). K562, a2780 and all the melanoma cell lines were cultured in RPMI 1640 medium (Life Technology, Milan, Italy) supplemented with penicillin (100 IU/mL) and streptomycin (100mg/mL) and 10% FBS. Huh7 and RKO cell lines were cultured in DMEM

medium (Life Technology, Milan, Italy) supplemented with penicillin (100 IU/mL) and streptomycin (100mg/mL) and 10% FBS. HDFa cell line was cultured DMEM medium (Life Technology, Milan, Italy) supplemented with penicillin (100 IU/mL) and streptomycin (100mg/mL) and 20% FBS. For all experiments, cells were used within two weeks after thawing.

Melanoma stem cell isolation from metastatic melanoma specimens and propagation was performed as previously described (26), in accordance with the ethical standards on human experimentation. Melanoma stem cells were constantly authenticated by using the short tandem repeat (STR) system (GlobalFilter STR Kit, Applied Biosystems, Foster City, CA, USA) followed by DNA sequencing (ABIPRISM 3130 genetic analyzer, Applied Biosystem). Cells, growing as multicellular spheres, were cultured in serum-free medium supplemented with epidermal growth factor (EGF, 20 ng/ml, PeproTech) and basic fibroblast growth factor (bFGF, 10 ng/ml, PeproTech), using ultra-low attachment flasks (Corning Incorporated, Corning, NY, USA). Melanoma stem cells were washed twice with PBS and cultured in attachment conditions in 10% FBS DMEM for at least 21 days to obtain sphere-derived adherent cells (SDAC).

To exclude mycoplasma infection, cells were routinely analyzed by the MycoAlert PLUS Mycoplasma Detection Kit (Lonza, Basel, Switzerland). In order to assess the sphere-forming capacity of CSCs, 1,000 cells/ml were plated in ultra-low attachment flasks. After 10 days, spheres that reached ≥ 50 μm of diameter were counted. In order to assess the tumorigenic capacity of CSCs, a total of 25×10^3 CSCs were suspended in serum-free medium 1:1 matrigel (BD Biosciences Pharmingen, San Diego, CA, USA) and subcutaneously injected into NOD/SCID mice. All the used cell lines were maintained in culture for no longer than 3 weeks and were not authenticated in the past year.

Immunofluorescence staining

Thawed PBMCs from metastatic melanoma patients and healthy donors, as well as fresh melanoma cells and CSCs, were subjected to immunofluorescence staining (Supplementary Table S2). The isotype-specific goat anti-mouse was from Southern Biotechnology (Birmingham, AL, USA). For NCR ligand detection, NKp30-Fc NKp46-Fc were obtained as previously described (27). After incubation, cells were washed twice with PBS 1X, resuspended in FACS Flow and acquired by FACS CANTO II, FACS ARIA I, Accuri C6 or a FACS Verse flow cytometer (BD Biosciences). 7 AAD Staining Solution (BD Biosciences) was added before each acquisition to distinguish between dead and live cells. In all the experiments, isotype-matched controls were used to set up the negative values. Data were analyzed using Flow-Jo version 10, version 9.3.1 software analysis (Treestar US, Ashland, OR, USA) or FacsSuite software (BD Biosciences).

CD107a mobilization assay after K562 pulsing

To quantify cell surface expression of CD107a, degranulation assays were performed. Thawed lymphocytes derived from 27 melanoma patients (4 stage III and 25 stage IV) and 18 healthy donors were cultured at 37°C in 5% CO2 in the presence of 8μL of PE-conjugated CD107a/IgG1 antibody (BD Biosciences) in U-bottom 96-well plates. After 1 h, Brefeldin A (10μg/mL) (Sigma Aldrich, Saint Louis, MO, USA) was added for 3 hours of incubation. Cells were then collected, washed with PBS 1X and stained with anti-CD56APC and anti-CD3FITC (Miltenyi Biotec) and acquired as described above.

NK and melanoma cell co-culture

Resting NK cells were cocultured at 37 °C in 5% CO2 with melanoma cells at 5:1 ratio in flat bottom 12-well plates (Corning Incorporated, Midland, NY, USA) supplied with 1640 RPMI (Life Technology, Milan, Italy) supplemented with penicillin (100 IU/mL) and streptomycin (100mg/mL) and 10% FBS. After 4 hours, cells were collected, stained and acquired as described above.

Cytotoxicity assays

Based on a protocol described elsewhere (28), cytotoxic assays were performed using fluorescent 5,6-carboxy-fluorescein-diacetate (CFDA). In brief, target cells were labeled with 150 μg/ml of CFDA-mixed isomers (Invitrogen) for 30 minutes and then incubated in 96-well U-bottom plates at 37°C in a humidified 5% CO2 incubator for 4h with freshly purified allogenic NK effector cells at different effector:target (E:T) ratios. Target cell specific lysis was analyzed by flow cytometry (FACS CANTO II and FACS ARIA I, BD Biosciences) and calculated as: % of specific lysis = (CT-TE)/CT*100, where CT indicates target cells' mean fluorescence in control tubes and TE indicates target cells' mean fluorescence in tubes containing effector cells. Data were collected and analyzed as described above.

Immunohistochemistry and Immunofluorescence staining

Hematoxylin & eosin staining was performed on paraffin-embedded sections of patient-derived primary melanoma, relative metastasis and xenograft tumor tissues, according to manufacturer's instructions.

Immunofluorescence staining was performed on 5-μm-thick embedded sections of human melanoma tissues and on melanoma CSCs cytospinned on glass slides. Cells were fixed in 2%

paraformaldehyde for 20 minutes at 37°C. Slides were exposed overnight at 4°C to CD44 (BU75, mouse IgG2a,k Ancell), CD271 (C40-1457, mouse IgG1a,k BD), ABCB5 (N13, goat IgG, SantaCruz), CD166 (MOG/07, mouse IgG2a,k, Novocastra), CCR7 (goat, Abcam), PD-L1 (mouse IgG1, R&D System), Gal-9 (rabbit IgG1, Thermo Scientific) or isotype matched controls IgG2a (mouse monoclonal Ancell), IgG1k (mouse BD), IgG (goat ThermoFischer Sceintific). Primary antibodies were revealed using Alexa Fluor-488 anti-rabbit, mouse or goat secondary antibodies. Nuclei were counterstained with Toto-3 iodide (Molecular Probes). In patient-derived primary melanoma and metastasis tissues, melanoma cells were distinguished from lymphocytes on the basis of cell morphology and size. Hematoxylin and eosin staining was performed by incubating sections with hematoxylin for 2 min and eosin for 1 min.

Microarray cytokine assay

To quantify serum cytokines, samples of thawed sera from 112 patients and 9 healthy donors were analyzed using the biochip analyzer Evidence Investigator (Randox Labs, Crumlin, UK) and the "Cytokine Array I" kit (Randox, Crumlin, UK), for the simultaneous quantification of the following cytokines: interleukin-2 (IL2), IL4, IL6, IL8, IL10, IL1a, IL1b, vascular endothelial growth factor (VEGF), interferon-g (IFNg), monocyte chemotactic protein-1 (MCP1), tumor necrosis factor-a (TNF-a), Epidermal Growth Factor (EGF). ELISA kits following manufacturer's instructions evaluated the concentrations of IL15, IL21, CCL19 and CCL21, in patients' serum and supernatants obtained from melanoma cell lines and melanoma CSC cultures; R&D Systems, Minneapolis, MN, USA for IL15, BioVendor, Brno, Czech Republic for IL21 and Aviva Systems Biology, San Diego, CA, USA for CCL19 and CCL21. Chemokine secretion from melanoma cells was assessed by measuring CCL19 and CCL21 concentration in 10 different melanoma cell lines and 7 melanoma CSCs using ELISA kits following manufacturer's instructions (Aviva Systems Biology).

Statistical analysis

Data obtained from multiple experiments were analyzed for statistical significance. Data from two related groups were analyzed using the paired Student's t-test or Wilcoxon signed rank test for samples that were or were not normally distributed, respectively. Data from two unrelated groups were analyzed using unpaired Student's t-test or Mann–Whitney test for samples that were or were not normally distributed, respectively. Data from three related groups were analyzed using a two-way analysis of variance (ANOVA) followed by Bonferroni's correction. Data from three unrelated groups were analyzed using one-way ANOVA followed by Bonferroni's correction or Kruskal-Wallis test followed by Dunn's correction for samples that were or were not normally distributed,

respectively. p-values < 0.05 were considered statistically significant. Kaplan–Meier (KM) curves were used to compare the survival of patients below or above median CCL19 serum concentration. The log-rank test was used to compare the KM curves and calculate the p-value. Statistical computations were performed using the GraphPad Prism 5.0 software.

Multivariate analysis

SIMCA, version 14 (MKS Data Analytics Solutions, Umeå, Sweden) was applied for multivariate analysis (29). A total of 85 variables, including immune profile and biographical variables, was applied in the analysis.

Orthogonal Projections to Latent Structures and Discriminant Analysis (OPLS-DA) was used to distinguish groups and identify parameters characterizing each group. As a development of classical principal component analysis, in OPLS-DA the systematic variation in the data is summarized into scores (T) that represent the systematic variation in the N-dimensional variable space related to a Y-variable outcome. In this projection method, all the variations related to the separation between groups are present in the predictive component(s) t[x], while the variation unrelated to separation between groups is visualized as “orthogonal components” to [x]. The contribution of each variable to the phenotype of each group of samples is indicated by the regression coefficient, that ranges from -1 (perfect negative correlation) to +1 (perfect positive correlation). OPLS-DA model quality is assessed by internal cross-validation, and presented as the percentage of data explained and predicted by the models. A good biological model is defined as having > 40% predictive capacity. The model was built on the basis of excluding biologically irrelevant and/or redundant variables (i.e. subsets with no signal) and screening for outliers (samples deviating significantly both from their own group and the global OPLS-DA model).

Results

Immune profiles of melanoma patients during disease progression

To investigate the correlation between immune variables and melanoma progression, the immune profile of PBLs from 42 healthy donors and 80 melanoma patients, grouped according to TNM classification of the American Joint Committee on Cancer (AJCC) (30) (stage III, n = 15; stage IV, n = 65) was analyzed by flow cytometry. Patients at stage IV were analyzed in a previous study (22); those profiles were used here to compare with immune profiles obtained from patients at stage III.

Data from the immune profiles, together with biographical variables (Supplementary Table S3), were used to create a multivariate model. Based on the Principal Component Analysis, Orthogonal Projections to Latent Structures Discriminant Analysis (OPLS-DA) evaluates all the variables simultaneously, giving them the same importance independent of the value range. This approach allows assessment and display of both the co-variation between variables and the correlation to a specific group of samples. Since the components are orthogonal, the difference between groups is represented by the first principal component (horizontal axis), whereas orthogonal components (vertical axis) stand for unrelated variation. Compared to traditional methods for statistical analysis, the advantage of using OPLS-DA models for biomarker identification is that a smaller cohort of patients is needed for the analysis.

The OPLS-DA model was built including only samples characterized for at least 50% of the variables considered. Thus, 37 healthy donors, 11 stage III and 42 stage IV melanoma patients were included. The OPLS-DA model gave a good separation between healthy donors and the two groups of patients (Fig. 1A), explaining 79% of the difference between them with a cross-validated predictive capacity of 69%. Overall, 66 variables contributed to distinguishing the groups. The ten most significant variables characterizing each group as well as the relative contribution of each characterizing variable are reported in Figures 1B-D.

The immune profile characteristic of healthy donor featured high frequency and expression of NKp46 on the $CD56^{dim}$ NK cell compartment. The stage III immune profile was characterized by high frequencies of chemokine receptors (CXCR2, CCR2) and NK activating receptors (NKG2D, NKp30, NKG2C). Stage IV melanoma patients were characterized by elevated percentages of CCR7 and CXCR2 on NK cells and high expression of inhibitory receptors (Tim-3, PD-1) on both NK and T cells.

Overall, the immune variables applied in the multivariate analysis identified separate groups and identified the variables best correlating with disease staging. Since the OPLS-DA identifies even those variables that are significant only when taken together with other parameters, variables

reported by the model were analyzed also in univariate mode to select biomarkers that remain significant even when considered on their own. The complete list of variables characterizing the immune profile of each group, together with the univariate validation, is reported in the Supplementary Table S4.

Functional analysis of T and NK cells from melanoma patients

The functional features of circulating NK and T cells at different disease stages were analyzed to understand their possible role in the pathophysiology of melanoma. Lymphocyte activation was investigated in a subset of patients. Representative plots for NK and T cells degranulation are showed in Figure 2A, B. NK cells from melanoma patients showed higher spontaneous degranulation compared to healthy donors (Fig. 2C). On the other hand, T cell degranulation was higher in stage IV melanoma patients compared to healthy donors (Fig. 2D).

Changes in CCR7^{+} CD56^{bright} NK cells and CCL19 mark disease evolution

To characterize cytokine profiles, sera from stage III and stage IV melanoma patients were analyzed and compared. Most of the stage IV melanoma patients had been previously characterized (22). The univariate analysis showed significant differences between stage III and IV for 5 out of 15 cytokines: CCL2, IL6, CXCL8, IL15 and CCL19. All the cytokines showed a steady longitudinal serum concentration increase paralleling melanoma disease clinical evolution. Since CCL2, CXCL8 and CCL19 reached the highest concentration at stage IV, we analyzed expression of their cognate receptors on both NK and T cell subpopulations (Supplementary Table S4). Among them, only the percentage of CCR7 on the CD56^{bright} NK cell subset displayed a pattern similar to the respective chemokine (Fig. 3A-B). Indeed, the frequency of CCR7^{+}CD56^{bright} NK cells reached its peak in stage IV melanoma patients, as did CCL19 concentration, suggesting an ectopic recruitment of this NK subset in the blood. Thus, this pathway may feature in melanoma progression.

The increased of CCL19 in sera may depend on its production by melanoma cells. Indeed, melanoma can produce IL8 and MCP-1 (31-33). Thus, we speculated that the high CCL19 observed in stage IV melanoma patients could be due to ectopic production from melanoma cells. To test this hypothesis, we measured CCL19 concentrations in supernatants from primary and metastatic melanoma cells, melanoma cancer stem cells (CSCs), fibroblasts and other solid tumors (hepatic, ovarian and colon carcinoma) cells. We observed CCL19 secretion by melanoma cells (Fig. 3C). Patient serum concentrations of the other four cytokines are listed in Supplementary Table S5. Serum concentrations of CCL2 exceeded the physiological range in all melanoma stages, whereas concentrations of the other three cytokines (IL6, CXCL8, IL15) reached pathological levels only in

stage IV melanoma. We previously demonstrated that melanoma cells produced CCL2, IL6 and CXCL8 (21). These soluble factors were found in culture supernatants of infiltrated lymph nodes from melanoma patients and were able to induce CCR7 expression on $CD56^{bright}$ NK cells (21). The IL15 cytokine induced phenotypic changes in NK cells from melanoma patients (22).

Melanoma cells susceptible to NK cell cytotoxicity express CCR7

CCR7 is a receptor involved in lymph node homing, and lymph nodes are the first anatomical sites vulnerable to melanoma metastatic spread. Therefore, we hypothesized that CCR7 could be ectopically expressed in melanoma metastatic cell lines, driving their lymph node metastatic colonization. Thus, we analyzed a panel of patient-derived melanoma cell lines for CCR7 expression. We also analyzed other surface molecules key to NK-melanoma cell cytotoxic synapse formation, such as MICA/B, PVR, HLA-class I, PD-L1, and Galectin-9. We analyzed ten melanoma cell lines of different anatomical origins. CCR7 was always expressed by a small fraction (1-5%) of melanoma cells (Fig. 4A) that appears to be a specific subpopulation. Indeed, such $CCR7^+$ melanoma cells co-expressed CCR7 with two immune checkpoints ligands, PD-L1 and Galectin-9 (Fig. 4A-B), recognized by PD-1 and Tim-3 on lymphocytes, respectively.

Thus, in each of ten different melanoma lines, a small fraction of cells expresses a chemokine receptor known for lymph node homing and also expresses PD-L1 and Galectin-9 that could protect from T and NK cell cytotoxic attack. Other molecules involved in NK cell cytotoxic synapses were measured. We found that $CCR7^+$ melanoma cells displayed low expression of MHC class I molecules and PVR, but high expression of NCR ligands (Fig. 4C). On the other hand, the activating ligands MICA/B and ULBP2, recognized by NKG2D, showed variable expression, being expressed on only four and six of the ten cell lines analyzed, respectively (Supplementary Fig. S1A-B). The low MHC class I and the high NCR ligands expression on $CCR7^+$ melanoma cell surface suggested an increased susceptibility to NK cell cytotoxicity.

To test whether NK cells could target $CCR7^+$ melanoma cells, we performed cell co-cultures using melanoma cells lines and NK cells. After co-culture with fresh NK cells, a reduction in the frequency of $CCR7^+PD\text{-}L1^+Galectin\text{-}9^+$ (referred as $CCR7^+$ cells) subpopulation was observed (Fig. 4D, left panel), whereas the $CCR7^-$ $PD\text{-}L1^-$ $Gal\text{-}9^-$ (referred as $CCR7^-$ cells) melanoma cell population was not affected by NK cell exposure (Fig. 4D, right panel). Furthermore, $CCR7^+$ melanoma cells that survived after the NK cells co-culture were found to express higher HLA-class I molecules levels (Supplementary Fig. S1C). PD-L1 expression was not affected by NK cells exposure, thus, ruling out the possible effect of IFNγ produced by NK cells (34) in the induction of MHC-class I molecules on the resistant $CCR7^+$ melanoma cells (Supplementary Fig. S1D).

CCR7 expression identifies melanoma CSCs susceptible to NK cell cytotoxicity

$CCR7^+$ melanoma cells are characterized by potentially higher migration capability, lower expression of membrane-associated MHC-class I molecules, low frequency within the bulk melanoma cell population, and increased susceptibility to NK cell-mediated killing. These features resemble those of CSCs (24, 35). To test the hypothesis that $CCR7^+$ melanoma cells are CSCs, we compared $CCR7^+$ cells to CSCs derived from melanoma generated with previously established methods (Table 1 and Fig. 5). First, we checked melanoma patient-derived CSCs for their ability to grow as spheres and to generate highly proliferating differentiated cells. We also tested for their aptitude to initiate tumor growth in immunocompromised mice (Fig. 5A-B). We showed that melanoma CSCs generated xenografts with histology typical of human melanomas (Fig. 5B). CSC stemness was confirmed by the expression of known stemness markers such as CD44, CD271, ABCB5 and CD166 (Fig. 5C and Supplementary Fig. S2A) (36-38). Finally, we measured the percentage of CSCs expressing CCR7 and observed that, in the four lines tested, CSCs homogenously expressed CCR7 (Fig 5D). PD-L1 and Galectin-9 were also expressed on CSCs but to a different extent (Supplementary Fig. S2B). Thus, CCR7 expression seems to identify CSCs.

Since we have previously demonstrated that human colon adenocarcinoma derived CSCs (25) and human and mouse breast adenocarcinoma CSCs (20) are susceptible to NK cell cytotoxic recognition, we evaluated melanoma CSC susceptibility to NK cell mediated lysis. Indeed, freshly purified NK cells showed an enhanced capability to recognize and kill melanoma-derived CSCs (Fig. 5E-G).

To summarize, well-defined melanoma cancer stem cells share a number of characteristics with the melanoma subpopulations explored in this paper: expression of CCR7, PD-L1 and Gal-9 as well as high susceptibility to NK cells. Thus, we hypothesize that this melanoma cell population plays a role in metastasis.

CCR7 is highly expressed in metastasis of melanoma patients

We then evaluated the clinical relevance of CCR7, Gal-9 and PD-L1 in the process of metastasis dissemination and outgrowth. Immunohistochemical analysis on tissues derived from patients who have melanoma metastases revealed the enrichment of $CCR7^+$ cells in melanoma metastatic lesions of the lymph node and parotid gland as compared to primary melanoma (Fig. 6A-C). Gal-9 and PD-$L1^+$ cells concomitantly expressed CCR7, suggesting that CCR7 is required for the metastatic outgrowth of aggressive melanoma cells (Fig. 6D).

We also analyzed the potential correlation between CCL19 serum concentrations and survival in a small cohort of patients. Our preliminary data (Supplementary Fig. S3) showed a tendency for a better overall survival in those patients who had less CCL19 in their blood; this observation needs to be validated in a larger patient cohort.

Discussion

Immune profile analysis of melanoma patients at different stages of disease progression suggests that melanoma progression leads to changes in peripheral blood NK and T cell subsets. In stage III melanoma, the NK cell compartment is dominated by subpopulations expressing CXCR2 and CCR2, both of which are receptors for the melanoma-produced chemokines IL8 and CCL2 (MCP-1), possibly indicating a more robust migration of NK cells in early-stage melanoma disease. Indeed, both IL8 and CCL2 act as a tumor autocrine growth factors increasing melanoma cell migration in metastatic lesions (39, 40). Thus, it is conceivable to speculate that these NK cell subsets may be able to migrate to the early melanoma metastatic foci. At this stage, circulating NK cell subsets expressing activating receptors (NKG2D, NKp30, NKG2C) prevail, whereas the T cell compartment is characterized by a reduced frequency of mature $CD57^{+}CD8^{+}$ cells associated with low levels of Tim-3 and CCR7. Circulating $CD56^{dim}$ NK cells in stage III melanoma patients appear to be activated and display basal degranulation without any stimulation *in vitro*. Later in the disease's evolution (stage IV), a similar feature is evident for T cells. This sequential activation, involving first the innate and then the adaptive immunity, recapitulates the physiological dynamics of the immune response.

On the other hand, stage IV melanoma is characterized by an increased frequency and accumulation of $CCR7^{+}$ $CD56^{bright}$ NK cells in patients' blood. This phenomenon could be due to the cumulative effects exerted by CCL2, IL6 and IL8, as previously demonstrated (21), whose serum concentrations are increased in the latest stage of the disease. Serum at stage IV has higher concentrations of the CCR7-ligand CCL19 than serum at stage III. The ectopic presence of CCL19, otherwise characteristic of lymph nodes, could be part of a pathogenic mechanism interfering with NK cell migration in melanoma infiltrated lymph nodes. T cells expressing CCR7, in contrast with $CD56^{bright}$ NK cells, did not increase in the blood of stage IV melanoma patients, suggesting that T cells may overcome the increased CCL19 sera concentration and redistribute to peripheral tissues. This could be explained by at least two, not mutually exclusive, mechanisms: (a) other lymph node homing receptors expressed by T cells, such as CD62L, could drive them to the lymph nodes independently of the CCR7-CCL19 axes, and (b) the cytokine milieu associated with stage IV melanoma (which includes IL6, CCL2 and IL8) does not induce CCR7 expression on T cells.

Blood NK cells from stage III and IV melanoma patients showed increased expression of CD107a when explanted to *in vitro* culture without further stimulus. This spontaneous degranulation may reflect the recent *in vivo* activation of the cells (that the cells have been in action recently *in vivo).* CD107a expression might thus mimic a "smoking gun" following the NK cell attack on circulating melanoma cells. However, there are other possible explanations, such as generalized activation of

NK cells by cytokines and other factors associated with advanced disease.

The scenario emerging from our study is that melanoma cells and related CSCs may produce CCL19, as described for cervical cancer (41). The increased serum concentration of CCL19 found in stage IV melanoma patients could be explained by the higher disease burden, where an increased number of CSCs actively secrete the chemokine. This could promote melanoma metastatic dissemination through at least two mechanisms: (1) CSCs migration from skin to blood circulation through the molecular combination between their CCR7 expression and the high patient's CCL19 blood concentration, (2) the high blood concentration of this chemokine, normally present only in the lymph nodes, retain $CD56^{bright}$ NK cells in the blood and prevent their progression to the lymph nodes, reducing their frequencies in the melanoma infiltrated lymph nodes as we have previously demonstrated (21). However, it is also possible that $CD56^{bright}$ NK cells resident in lymph nodes may be rerouted to the blood. Indeed, studies indicate that crosstalk between NK cells and DCs in the lymph nodes affects the $CD8^+$ T cell anti-tumor immune response, as reviewed elsewhere (42, 43). NK cells can edit the DC population (1) by physical elimination of immature DC or (2) by IFNγ production that induces full maturation of the DC skewing toward a Th1 immune response (44, 45). Thus, we speculate that the perturbation in $CD56^{bright}$ NK cell migration in the lymph nodes may contribute to the failure of the anti-tumor immune response in the late stage of melanoma disease. Our data complement findings demonstrating that NK cell frequencies in melanoma tissues positively correlate with anti-PD-1 immunotherapy and overall survival (46). Regardless of the pathological meaning of CCL19 concetration and the accumulation of $CCR7^+CD56^{bright}$ NK cells in the blood circulation, our study demonstrates concomitant expression of CCR7 on melanoma CSCs and NK cells and that NK cells can recognize and eliminate melanoma CSCs that drive the disease's metastatic spread.

Ex vivo analysis showed that CCR7 is expressed more in metastatic melanoma cells than in melanoma cells at the primary tumor site. These data corroborate and expand previously reported findings (47, 48), suggesting that melanoma cells rely on CCR7 during metastasis.

Moreover, Gal-9^+ and PD-$L1^+$ melanoma cells concurrently expressed CCR7 showing the presence of an aggressive subpopulation of $CCR7^+$ cells endowed with immune evasion capabilities. Our results provide a foundation for developing melanoma therapies that could interfere with this metastatic pathway by the use of monoclonal antibodies targeting CCL19.

Acknowledgments

S. Pesce is recipient of a fellowship awarded by Fondazione Umberto Veronesi. A. Turdo is a recipient of an AIRC fellowship.

We thank Claudia Cantoni (University of Genoa and Istituto Giannina Gaslini, Genoa) for supplying the NKp30-Fc and NKp46-Fc fusion protein.

Author contributions

C.M.C. and A.T. performed the experiments, analyses and manuscript writing, V.V. performed the experiments, T.A. performed experiments, M.C., G.M., D.M., A.M.G., sampling and clinical data collection, C.G., E.D.G, R.T., performed experiments, and sorting, E.M., S.P., G.D.Z. performed the experiments and analyses, V.A., F.S.C., E.G., were involved in data analyses, A.M, data analyses and interpretation, K.K., data analyses, interpretation and manuscript writing, A.R. immunohistochemistry and immunofluorescence staining, data analyses, P.A.A. was involved in sample collection, clinical data collection, manuscript writing, M.T. analyzed the data, wrote the manuscript, supervise the CSC part of the study, E.C. conceived the study, analyzed the data, wrote the manuscript, and designed the experiments. All the authors critically read and approved the manuscript.

References

1. Wolchok JD, Chiarion-Sileni V, Gonzalez R, Rutkowski P, Grob JJ, Cowey CL, et al. Overall Survival with Combined Nivolumab and Ipilimumab in Advanced Melanoma. The New England journal of medicine 2017;377(14):1345-56.
2. Hodi FS, Chesney J, Pavlick AC, Robert C, Grossmann KF, McDermott DF, et al. Combined nivolumab and ipilimumab versus ipilimumab alone in patients with advanced melanoma: 2-year overall survival outcomes in a multicentre, randomised, controlled, phase 2 trial. The Lancet Oncology 2016;17(11):1558-68.
3. Shain AH, Yeh I, Kovalyshyn I, Sriharan A, Talevich E, Gagnon A, et al. The Genetic Evolution of Melanoma from Precursor Lesions. The New England journal of medicine 2015;373(20):1926-36.
4. Al-Hajj M, Wicha MS, Benito-Hernandez A, Morrison SJ, Clarke MF. Prospective identification of tumorigenic breast cancer cells. Proceedings of the National Academy of Sciences of the United States of America 2003;100(7):3983-8.
5. Singh SK, Hawkins C, Clarke ID, Squire JA, Bayani J, Hide T, et al. Identification of human brain tumour initiating cells. Nature 2004;432(7015):396-401.
6. Ricci-Vitiani L, Lombardi DG, Pilozzi E, Biffoni M, Todaro M, Peschle C, et al. Identification and expansion of human colon-cancer-initiating cells. Nature 2007;445(7123):111-5.
7. Lacalle RA, Blanco R, Carmona-Rodriguez L, Martin-Leal A, Mira E, Manes S. Chemokine Receptor Signaling and the Hallmarks of Cancer. International review of cell and molecular biology 2017;331:181-244.
8. Spits H, Di Santo JP. The expanding family of innate lymphoid cells: regulators and effectors of immunity and tissue remodeling. Nature immunology 2011;12(1):21-7.
9. Vesely MD, Kershaw MH, Schreiber RD, Smyth MJ. Natural innate and adaptive immunity to cancer. Annual review of immunology 2011;29:235-71.
10. Sandel MH, Speetjens FM, Menon AG, Albertsson PA, Basse PH, Hokland M, et al. Natural killer cells infiltrating colorectal cancer and MHC class I expression. Molecular immunology 2005;42(4):541-6.
11. Richards JO, Chang X, Blaser BW, Caligiuri MA, Zheng P, Liu Y. Tumor growth impedes natural-killer-cell maturation in the bone marrow. Blood 2006;108(1):246-52.
12. Lopez-Soto A, Gonzalez S, Smyth MJ, Galluzzi L. Control of Metastasis by NK Cells. Cancer cell 2017;32(2):135-54.
13. Burke S, Lakshmikanth T, Colucci F, Carbone E. New views on natural killer cell-based immunotherapy for melanoma treatment. Trends in immunology 2010;31(9):339-45.
14. Lakshmikanth T, Burke S, Ali TH, Kimpfler S, Ursini F, Ruggeri L, et al. NCRs and DNAM-1 mediate NK cell recognition and lysis of human and mouse melanoma cell lines in vitro and in vivo. The Journal of clinical investigation 2009;119(5):1251-63.
15. Sottile R, Pangigadde PN, Tan T, Anichini A, Sabbatino F, Trecroci F, et al. HLA class I downregulation is associated with enhanced NK-cell killing of melanoma cells with acquired drug resistance to BRAF inhibitors. European journal of immunology 2016;46(2):409-19.
16. Sivori S, Carlomagno S, Pesce S, Moretta A, Vitale M, Marcenaro E. TLR/NCR/KIR: Which One to Use and When? Frontiers in immunology 2014;5:105.
17. Cooper MA, Fehniger TA, Caligiuri MA. The biology of human natural killer-cell subsets. Trends in immunology 2001;22(11):633-40.

18. Freud AG, Mundy-Bosse BL, Yu J, Caligiuri MA. The Broad Spectrum of Human Natural Killer Cell Diversity. Immunity 2017;47(5):820-33.
19. Pesce S, Greppi M, Tabellini G, Rampinelli F, Parolini S, Olive D, et al. Identification of a subset of human natural killer cells expressing high levels of programmed death 1: A phenotypic and functional characterization. The Journal of allergy and clinical immunology 2017;139(1):335-46 e3.
20. Vivier E, Raulet DH, Moretta A, Caligiuri MA, Zitvogel L, Lanier LL, et al. Innate or adaptive immunity? The example of natural killer cells. Science 2011;331(6013):44-9.
21. Ali TH, Pisanti S, Ciaglia E, Mortarini R, Anichini A, Garofalo C, et al. Enrichment of CD56(dim)KIR + CD57 + highly cytotoxic NK cells in tumour-infiltrated lymph nodes of melanoma patients. Nature communications 2014;5:5639.
22. Tallerico R, Cristiani CM, Staaf E, Garofalo C, Sottile R, Capone M, et al. IL-15, TIM-3 and NK cells subsets predict responsiveness to anti-CTLA-4 treatment in melanoma patients. Oncoimmunology 2017;6(2):e1261242.
23. Tallerico R, Conti L, Lanzardo S, Sottile R, Garofalo C, Wagner AK, et al. NK cells control breast cancer and related cancer stem cell hematological spread. Oncoimmunology 2017;6(3):e1284718.
24. Tallerico R, Garofalo C, Carbone E. A New Biological Feature of Natural Killer Cells: The Recognition of Solid Tumor-Derived Cancer Stem Cells. Frontiers in immunology 2016;7:179.
25. Tallerico R, Todaro M, Di Franco S, Maccalli C, Garofalo C, Sottile R, et al. Human NK cells selective targeting of colon cancer-initiating cells: a role for natural cytotoxicity receptors and MHC class I molecules. Journal of immunology 2013;190(5):2381-90.
26. Todaro M, Alea MP, Di Stefano AB, Cammareri P, Vermeulen L, Iovino F, et al. Colon cancer stem cells dictate tumor growth and resist cell death by production of interleukin-4. Cell stem cell 2007;1(4):389-402.
27. Pesce S, Thoren FB, Cantoni C, Prato C, Moretta L, Moretta A, et al. The Innate Immune Cross Talk between NK Cells and Eosinophils Is Regulated by the Interaction of Natural Cytotoxicity Receptors with Eosinophil Surface Ligands. Frontiers in immunology 2017;8:510.
28. McGinnes K, Chapman G, Marks R, Penny R. A fluorescence NK assay using flow cytometry. Journal of immunological methods 1986;86(1):7-15.
29. Trygg J, Wold S. Orthogonal Projections to Latent Structures (O-PLS). Chemometrics 2002;16:119-28.
30. Gershenwald JE, Scolyer RA, Hess KR, Sondak VK, Long GV, Ross MI, et al. Melanoma staging: Evidence-based changes in the American Joint Committee on Cancer eighth edition cancer staging manual. CA: a cancer journal for clinicians 2017;67(6):472-92.
31. Scheibenbogen C, Mohler T, Haefele J, Hunstein W, Keilholz U. Serum interleukin-8 (IL-8) is elevated in patients with metastatic melanoma and correlates with tumour load. Melanoma research 1995;5(3):179-81.
32. Schadendorf D, Moller A, Algermissen B, Worm M, Sticherling M, Czarnetzki BM. IL-8 produced by human malignant melanoma cells in vitro is an essential autocrine growth factor. Journal of immunology 1993;151(5):2667-75.
33. Gatti L, Sevko A, De Cesare M, Arrighetti N, Manenti G, Ciusani E, et al. Histone deacetylase inhibitor-temozolomide co-treatment inhibits melanoma growth through suppression of Chemokine (C-C motif) ligand 2-driven signals. Oncotarget 2014;5(12):4516-28.
34. Taube JM, Anders RA, Young GD, Xu H, Sharma R, McMiller TL, et al. Colocalization of inflammatory response with B7-h1 expression in human melanocytic lesions supports an adaptive resistance mechanism of immune escape. Science translational medicine 2012;4(127):127ra37.

35. Di Tomaso T, Mazzoleni S, Wang E, Sovena G, Clavenna D, Franzin A, et al. Immunobiological characterization of cancer stem cells isolated from glioblastoma patients. Clinical cancer research : an official journal of the American Association for Cancer Research 2010;16(3):800-13.
36. Boiko AD, Razorenova OV, van de Rijn M, Swetter SM, Johnson DL, Ly DP, et al. Human melanoma-initiating cells express neural crest nerve growth factor receptor CD271. Nature 2010;466(7302):133-7.
37. Quintana E, Shackleton M, Foster HR, Fullen DR, Sabel MS, Johnson TM, et al. Phenotypic heterogeneity among tumorigenic melanoma cells from patients that is reversible and not hierarchically organized. Cancer cell 2010;18(5):510-23.
38. Klein WM, Wu BP, Zhao S, Wu H, Klein-Szanto AJ, Tahan SR. Increased expression of stem cell markers in malignant melanoma. Modern pathology : an official journal of the United States and Canadian Academy of Pathology, Inc 2007;20(1):102-7.
39. Uen WC, Hsieh CH, Tseng TT, Jiang SS, Tseng JC, Lee SC. Anchorage independency promoted tumor malignancy of melanoma cells under reattachment through elevated interleukin-8 and CXC chemokine receptor 1 expression. Melanoma research 2015;25(1):35-46.
40. Vergani E, Di Guardo L, Dugo M, Rigoletto S, Tragni G, Ruggeri R, et al. Overcoming melanoma resistance to vemurafenib by targeting CCL2-induced miR-34a, miR-100 and miR-125b. Oncotarget 2016;7(4):4428-41.
41. Zhang X, Wang Y, Cao Y, Zhang X, Zhao H. Increased CCL19 expression is associated with progression in cervical cancer. Oncotarget 2017;8(43):73817-25.
42. Kalinski P, Mailliard RB, Giermasz A, Zeh HJ, Basse P, Bartlett DL, et al. Natural killer-dendritic cell cross-talk in cancer immunotherapy. Expert opinion on biological therapy 2005;5(10):1303-15.
43. Lee SC, Srivastava RM, Lopez-Albaitero A, Ferrone S, Ferris RL. Natural killer (NK): dendritic cell (DC) cross talk induced by therapeutic monoclonal antibody triggers tumor antigen-specific T cell immunity. Immunologic research 2011;50(2-3):248-54.
44. Moretta A. Natural killer cells and dendritic cells: rendezvous in abused tissues. Nature reviews Immunology 2002;2(12):957-64.
45. Carbone E, Terrazzano G, Ruggiero G, Zanzi D, Ottaiano A, Manzo C, et al. Recognition of autologous dendritic cells by human NK cells. European journal of immunology 1999;29(12):4022-9.
46. Barry KC, Hsu J, Broz ML, Cueto FJ, Binnewies M, Combes AJ, et al. A natural killer-dendritic cell axis defines checkpoint therapy-responsive tumor microenvironments. Nature medicine 2018;24(8):1178-91.
47. Takeuchi H, Fujimoto A, Tanaka M, Yamano T, Hsueh E, Hoon DS. CCL21 chemokine regulates chemokine receptor CCR7 bearing malignant melanoma cells. Clinical cancer research : an official journal of the American Association for Cancer Research 2004;10(7):2351-8.
48. Takekoshi T, Fang L, Paragh G, Hwang ST. CCR7-expressing B16 melanoma cells downregulate interferon-gamma-mediated inflammation and increase lymphangiogenesis in the tumor microenvironment. Oncogenesis 2012;1:e9.

Sample	*Stage*	*Type of melanoma metastasis*	*Sphere forming*	*Xenograft*
CSC#1	IV	Unknown	Yes	Yes
CSC#2	IV	Lung	Yes	Yes
CSC#3	IV	Lung	Yes	Yes
CSC#4	IV	Lymph node	Yes	Yes

Table 1. Case description and sphere forming/tumorigenic capacity of melanoma stem cells.

Figure legends

Figure 1. Discriminant analysis of healthy donors and melanoma patients.

(A) Light grey dots = healthy donors (37), dark grey dots = stage III melanoma patients (11), black dots = stage IV melanoma patients (42). Horizontal axis = predictive component. Vertical axis = Orthogonal component not related to difference between groups. Ellipse = Hotelling's T2 95 % confidence interval limit. **(B-D)** 10 most significant variables correlated to healthy donors, stage III and stage IV melanoma patients, respectively. Regression coefficient represents relative contribution magnitude of each variable. Error bars = 95 % confidence intervals.

Figure 2. Analysis of NK and T cell function in healthy donors and melanoma patients.

(A-B) Representative dot plots of CD107a degranulation by NK **(A)** and T cells **(B)** from healthy donor (left panels), stage III (middle panels) and stage IV (right panels) melanoma patients. **(C-D)** Statistical analysis of CD107a degranulation by NK **(C)** and T cells **(D)** obtained from 18 healthy donors (white bars), 4 stage III (grey bars) and 25 stage IV (black bars) melanoma patients. The assay was performed once per sample. Analyses were performed Kruskal-Wallis test followed by Dunn's correction. ***p-value < 0.001; **p-value < 0.01.

Figure 3. CCR7 and CCL19 in melanoma patients.

(A-B) Circles = healthy donors; squares = stage III melanoma patients, triangles = stage IV melanoma patients. **(A)** Frequency of $CCR7^{+}CD56^{bright}$NK cells in 42 healthy donors, 15 stage III and 65 stage IV melanoma patients. Immunoprofile was performed once per sample. **(B)** Serum concentration of CCL19 in 9 healthy donors, 14 stage III and 22 stage IV melanoma patients. Measurement was performed in duplicate once per sample. **(C)** Mean CCL19 concentrations measured during the 48-120 hours timeframe in supernatants from fibroblast (circles, n = 1), solid tumor (squares, n = 3) primary and metastatic melanoma (diamonds, n =10; white indicate cells

derived from primary lesions, black diamonds indicate cells derived from metastatic lesions) and melanoma cancer stem cell lines (triangles, n = 7). Histological origin of melanoma cell lines is reported in Supplementary Table S1. For each time point, 3 independent experiments were performed in duplicate. Data are shown as mean ± SD. Analyses were performed by Kruskal-Wallis test followed by Dunn's correction **(A-C)** or ANOVA followed by Bonferroni's correction **(B)**. ***p-value < 0.001; # p-value ≤ 0.1

Figure 4. NK-mediated targeting of CCR7$^+$ melanoma cells.

(A) Representative plot of CCR7 frequency in melanoma cells and differential distribution of PD-L1 and Galectin-9 in CCR7$^-$ and CCR7$^+$ melanoma cells. **(B)** Frequency of the indicated molecules on CCR7$^-$ (white bars) and CCR7$^+$ (black bars) melanoma cells. Data refer to 10 different cell lines, for each of which measures were repeated in three independent experiments. **(C)** Expression of the indicated molecules on CCR7$^-$ (white bars) and CCR7$^+$ (black bars) melanoma cells Data refer to 10 different cell lines, for each of which measures were repeated in three independent experiments, and are shown as mean ± SD. The two melanoma cell subpopulations, CCR7$^-$ and CCR7$^+$ cells, were gated as reported in panel A. For NKp30-L and NKp46-L detection, NKp30-Fc NKp46-Fc were used in indirect immunofluorescent stainings, whereas direct immunofluorescent staining was used to detect the other indicated molecules. Based on distribution, analysis was performed by Student's paired t-test or Wilcoxon signed rank test. **(D)** Percentage of surviving CCR7$^+$ (left panel) and CCR7$^-$ (right panel) melanoma cells before (white bars) and after (black bars) co-culture with circulating freshly purified allogenic NK cells. Data deriving from four independent experiments are shown as mean ± SD. Analysis was performed by paired Student's t-test. ***p-value < 0.001; **p-value < 0.01; *p-value <0.05.

Figure 5. Primary melanoma cells and CSC susceptibility to NK-mediated killing.

(A) Sphere-derived adherent cells (SDAC) formation from melanoma stem cells. **(B)** Hematoxylin and eosin (H&E) staining, with respective magnification, of tumors generated by subcutaneous injection of patient-derived melanoma stem cells in NOD SCID immunocompromised mice. **(C)** Confocal microscopy analysis of the expression of stemness surface markers (CD44, CD271, ABCB5 and CD166) on primary melanoma-derived CSCs; the reported markers are labeled in green; nuclei are labeled in blue (Toto-3). **(D)** Frequency of CCR7$^+$ cells within melanoma cells (white bar) and CSCs (black bar). Data deriving from 10 primary melanoma cells and 4 CSCs are shown. **(E, F)** Cytotoxicity assays performed by culturing primary melanoma cells **(E)** and CSCs **(F)** with circulating freshly purified allogeneic NK cells used at different E:T ratios, as reported on

the x-axis. **(G)** Statistical analysis of the data obtained from at least two independent cytotoxicity experiments for each tested cell line at two E:T ratios. Data are shown as mean ± SD. Analysis was performed by Mann-Whitney test; **p-value < 0.01, *p-value < 0.05.

Figure 6. Metastatic melanoma cells express high amounts of CCR7.

(A-C) Representative hematoxylin and eosin staining (*Left panels*) and immunofluorescence analysis of CCR7 (green color), Gal-9 (red color) and PD-L1 (red color) (*Middle and Right panels*) on paraffin-embedded sections of primary melanomas and relative metastasis. **(A)** Primary melanoma of the scalp and its micrometastasis to the mastoid lymph node, **(B)** frontoparietal melanoma and its metastasis to the parotid and **(C)** primary nasopharynx melanoma and its submandibular lymph node metastasis. Toto-3 (blue) stains the nuclei. White arrowheads indicate melanoma cells expressing both CCR7 and PD-L1 or CCR7 and Gal-9. Scale bar represents 40 µm. **(D)** Percentage of melanoma cells expressing CCR7, CCR7/Gal9 and CCR7/PD-L1 in primary melanomas and paired metastatic sites as described in **(A-C)**. Data are shown as mean of 5 different fields counted for each sample ± SD. Analysis was performed by Mann–Whitney test; ***p-value < 0.001.

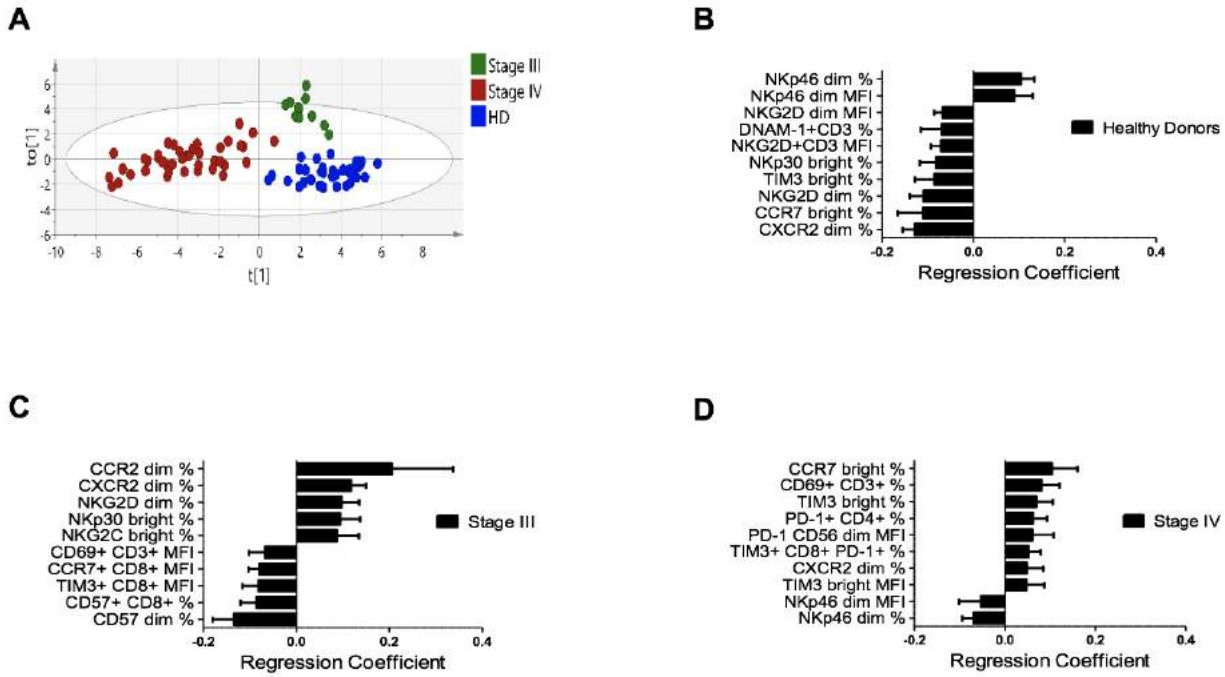

Figure 1

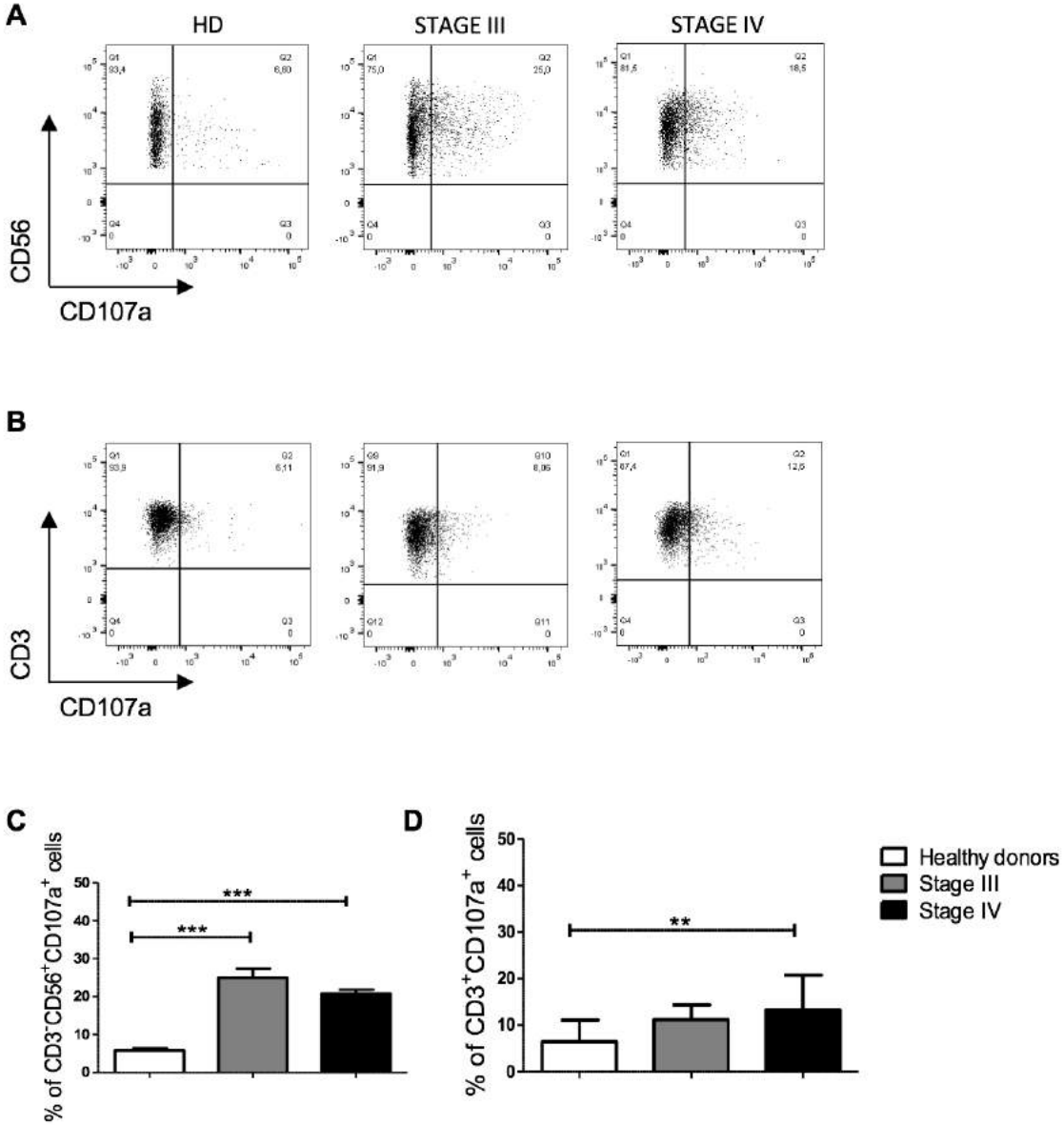

Figure 2

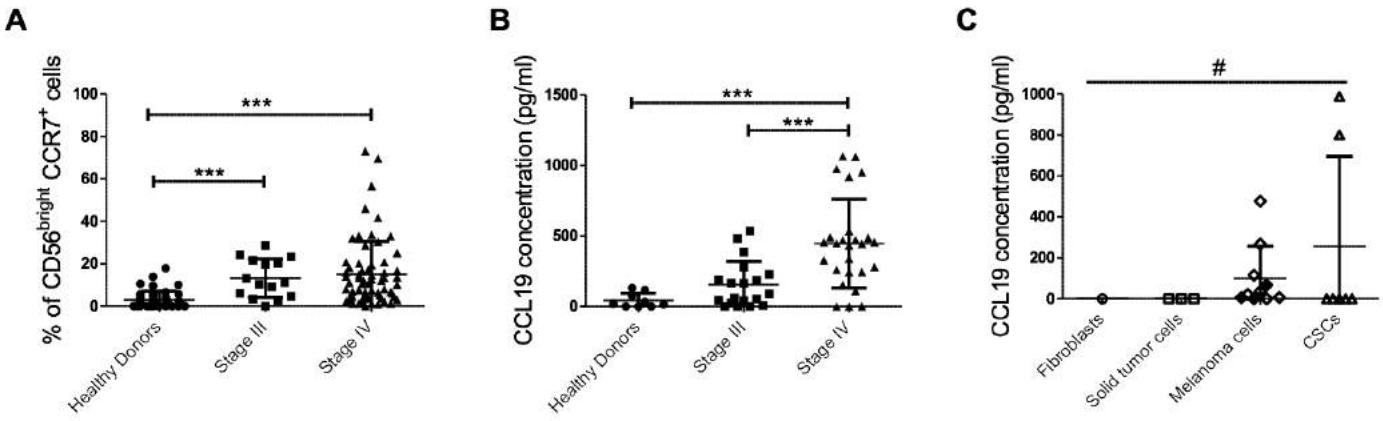

Figure 3

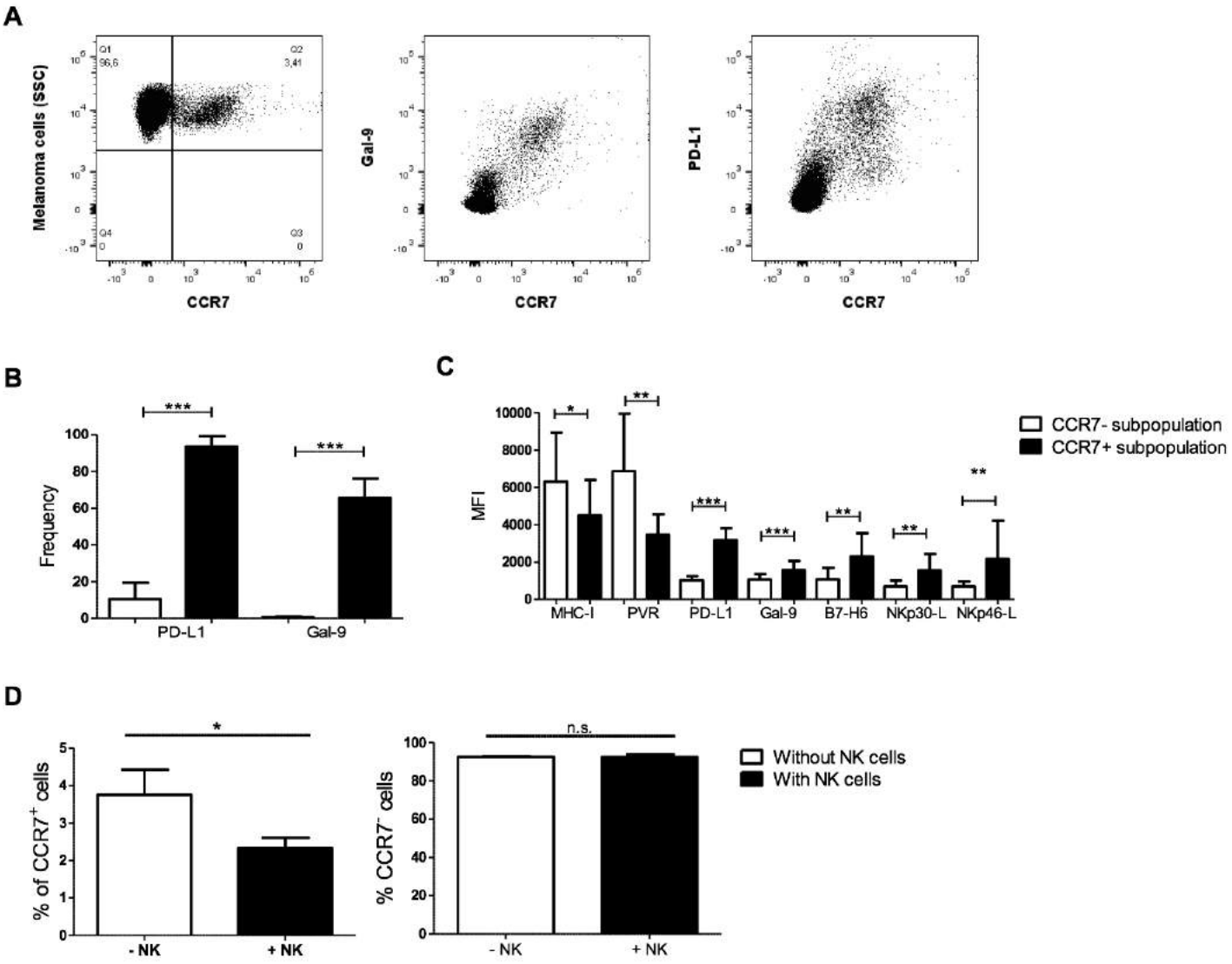

Figure 4

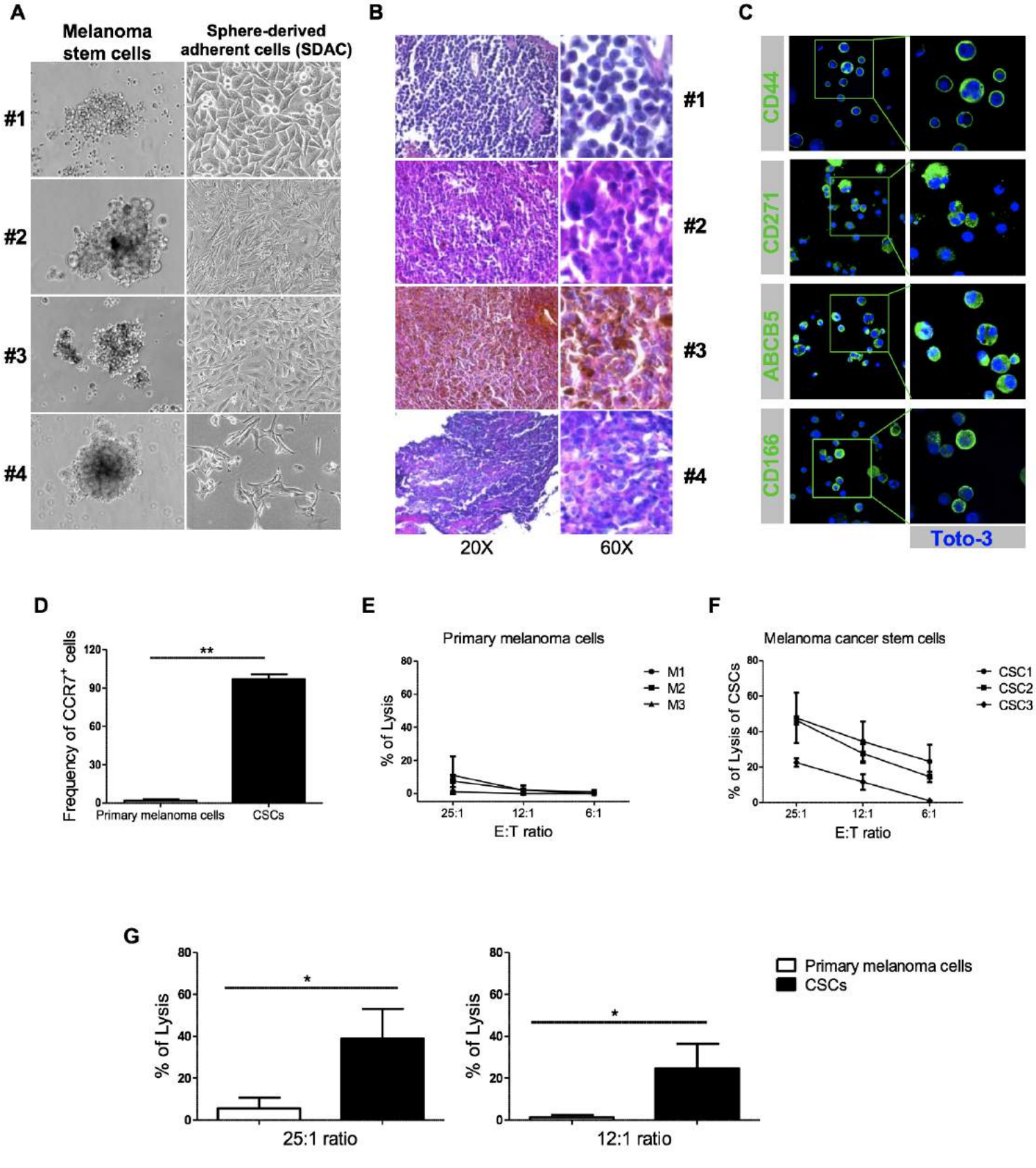

Figure 5

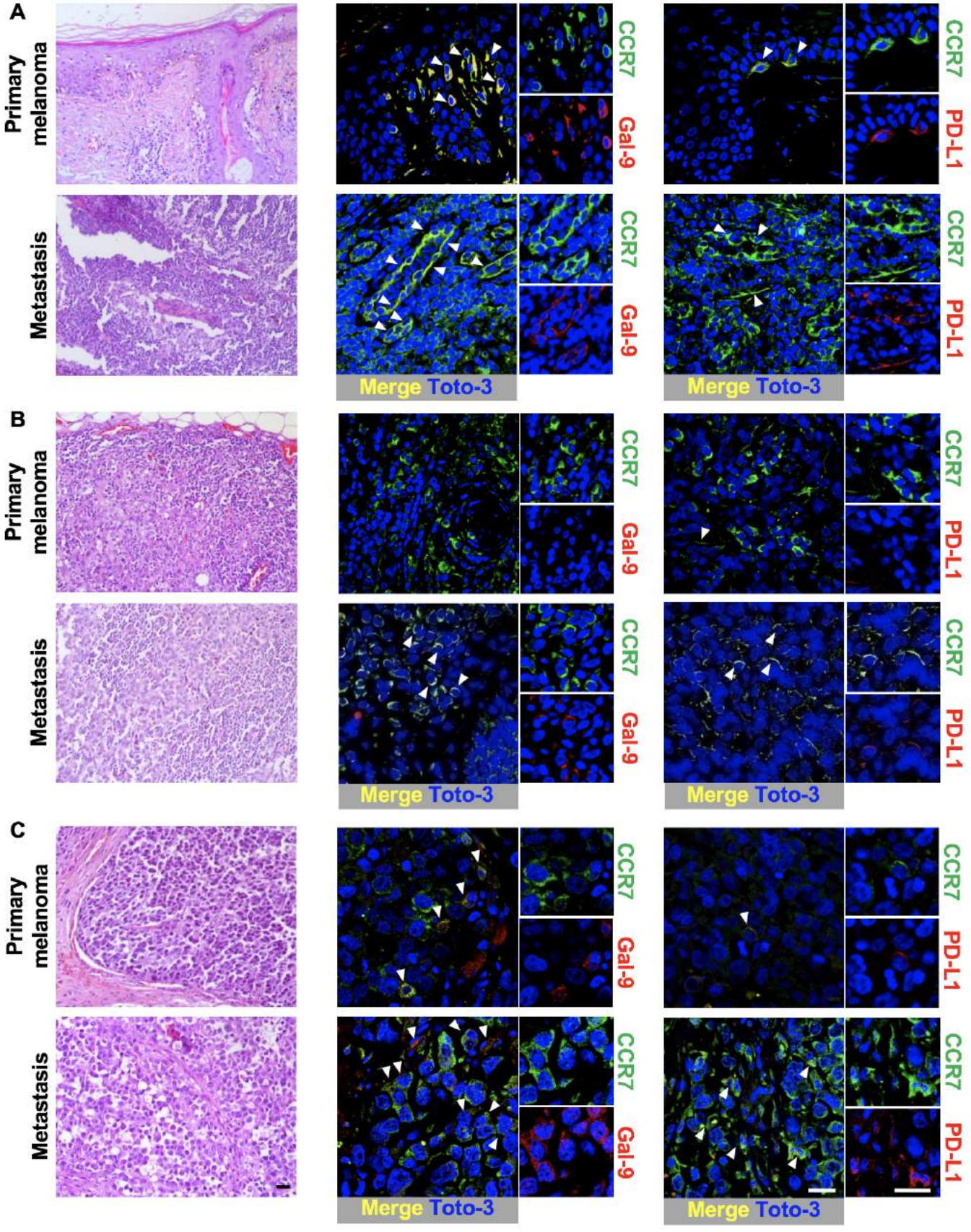

Figure 6

AACR American Association for Cancer Research

Cancer Immunology Research

Accumulation of circulating CCR7+ natural killer cells marks melanoma evolution and reveals a CCL19-dependent metastatic pathway

Costanza Maria Cristiani, Alice Turdo, Valeria Ventura, et al.

Cancer Immunol Res Published OnlineFirst April 2, 2019.

Print Email

Date: 2019-03-29 16:58:42

Last Sent: 2019-03-29 16:58:42

Triggered By: Redacted

BCC: Redacted

Subject: Decision Rendered: CIR-18-0651R1

Message: Re: CIR-18-0651R1

In melanoma patients the high frequency of circulating CCR7+ Natural Killer cells marks the disease evolution and reveals a new CCL19 dependent metastatic pathway.

Dear Dr. Carbone:

I am pleased to inform you that your above-referenced manuscript is acceptable for publication in CANCER IMMUNOLOGY RESEARCH.

You will receive your proofs electronically within 10-14 days. If you expect your e-mail address to change within this period of time please notify us immediately by writing to cancerimmunolres@aacr.org. The e-mail you will receive will include detailed information about marking and returning your proofs. Please read, correct, and return proofs within 2 business days (the schedule takes weekends and holidays into consideration).

IMPORTANT: Please note that if proofs are not returned within this time frame, publication of the article may be delayed until the next available issue.

Please also note that the assignment to which section of the journal your article will appear is made at the Editors' discretion.

We would like to call your attention to the following:

ONLINE FIRST:
Please note that all AACR journals now offer OnlineFirst publication of accepted manuscripts. The version of the manuscript which will be used for OnlineFirst publication is the PDF version of the manuscript which has been peer reviewed but not yet copyedited or typeset. Please review your accepted manuscript now and reply to this message within 48 hours if you object to having your accepted manuscript posted online in its present form. After proof corrections have been returned, the final edited version of your manuscript, incorporating any corrections or changes made at the proof stage, will replace the manuscript version online. Therefore, it is imperative that you return your corrected proofs as quickly as possible.

CHANGES IN PROOF:
Changes in proofs entail considerable expense and publication delay and thus are discouraged unless absolutely necessary. Authors will be charged for excessive alterations made in proof.

ARCHIVING MANDATES:
AACR journals can help you to fulfill many funders' mandates to archive your accepted manuscript by depositing your manuscript for you in PubMed Central (PMC) or Europe PubMed Central (Europe PMC). If your research is funded by the National Institutes of Health, Howard Hughes Medical Institute, Wellcome Trust, Cancer Research UK, and/or the Medical Research Council, AND IF YOU SELECTED THE ARCHIVING OPTION WHEN YOU SUBMITTED YOUR PAPER, you need to do nothing else.

If you did not select the archiving option and now wish to make use of the AACR journals' archiving service for authors, please contact the CANCER IMMUNOLOGY RESEARCH Editorial Office (cancerimmunolres@aacr.org) for assistance.

More information about AACR archiving, copyright, and permission policies is available at http://www.aacrjournals.org/site/InstrAuthors/ifora.xhtml#mandatesassist.

MEDIA COVERAGE:
If your internal Public Relations (PR) office plans a news release or other PR-related activity for this paper, please send an e-mail to julia.gunther@aacr.org. A member of the AACR Communications Team will liaise with your internal PR office to make sure embargo policies are followed.

Thank you in advance for your cooperation.

Sincerely,
Linda J. Miller, PhD
(for the Editors)
Executive Editor
Cancer Immunology Research